Journal of Catalysis 274 (2010) 221–227

Contents lists available at ScienceDirect

Journal of Catalysis

journal homepage: www.elsevier.com/locate/jcat

Facile one-pot approach to the synthesis of chiral periodic mesoporous organosilicas SBA-15-type materials

Rafael A. Garcia *, Rafael van Grieken, Jose Iglesias, Victoria Morales, Nelson Villajos

Department of Chemical and Environmental Technology, ESCET, Universidad Rey Juan Carlos, C/Tulipán s/n, 28933 Móstoles, Madrid, Spain

ARTICLE INFO

Article history:
Received 2 April 2010
Revised 2 July 2010
Accepted 2 July 2010
Available online 5 August 2010

Keywords:
Chiral PMOs
SBA-15
Tartrate derivatives
Asymmetric synthesis
Enantioselectivity

ABSTRACT

The synthesis of a chiral PMO SBA-15-type material from 100% purely organic monomers, 1,2-bis(triethoxysilyl)ethane and bis-silylated chiral ligands, by an easy one-pot methodology has been studied. Furthermore, these chiral periodic mesoporous solid materials with an incorporation as high as 50 mol% of dimethyl tartrate-derived chiral auxiliary precursor (Sharpless ligand) have been synthesized, without any reduction in the textural properties with reference to the ordering of the material. FTIR and NMR solid-state techniques confirm the presence of the chiral organic precursor in the SBA-15-type material framework. The thioanisole asymmetric oxidation reaction has been used to validate the heterogeneously synthesized catalyst activity, achieving moderate enantiomeric excess (ee) and satisfactory yield to sulfoxide up to 30% and 71%, respectively, corroborating the inclusion of the chiral tartrate moiety into the inorganic silica framework.

1. Introduction

Chiral periodic mesoporous organosilicates have been recently developed as a variety of periodic mesoporous organosiliceous materials (PMOs). Insertion of chirality inside the PMOs constitutes a breakthrough for potential applications particularly as catalysts for asymmetric synthesis. Hence, the development of novel heterogeneous chiral ligands that could effectively induce asymmetry might be crucial not only in organic synthesis, but it could allow the preparation of new valuable materials for applications in areas such as adsorption, chromatography, optical devices, and sensors [1–9]. The chiral PMO synthesis is accomplished through anchoring of chiral building blocks into the three-dimensional mesoporous framework of the silica matrix, in which the bis-silylated chiral organosilica precursors are homogenously distributed along the pore walls, playing the role of organic bridges in the silica network. These materials are characterized by a periodically organized pore system with a defined pore diameter.

Pioneering work with an organic chiral auxiliary incorporated into the framework of a MCM-41 inorganic material date from 2003, in which Garcia and co-workers develop a chiral PMO MCM-41-based material from a mixture of chiral bis-silylated binaphthyl or cyclohexadienyl precursor and tetraethoxysilane (TEOS) as the sources of silica, under basic conditions [10]. Accordingly, the chiral solid material was not purely PMOs, incorporating a maximum content of chiral precursor around 15 wt% without distorting the mesostructure. From this development, different groups have reported synthesis of chiral PMOs with several chiral precursor moieties, such as bis-silylated vanadyl salen complexes, chiral diurea ligands, BINOL and BINAP auxiliaries and chiral tartrate derivatives [11–18] extending the range of the applications. A common feature in all these works is that TEOS is needed as silica co-precursor to achieve the mesoscopic structure, which leads to rather small chiral functionality loadings. In addition, ionic surfactants are used as template, and therefore, MCM-41-like framework materials are obtained. Subsequently, some investigations dealing with the preparation of pure chiral mesoporous materials with only organic monomers, that is, without TEOS as silica co-precursor, have been published [19–22]. However, these works about the preparation of PMOs from 100% chiral bis-silylated functionalities demonstrate the lack of mesoscopic ordering in the final materials. Also, Fröba and co-workers have recently reported the synthesis of chiral periodic mesoporous organosilica in the presence of non-ionic oligomeric surfactant as the supramolecular structure-directing agent under acidic conditions [23]. Brij 76 was used as the template, leading to chiral benzylic ether-bridged hybrid material with a high surface area. Finally, using the same surfactant, MacQuarrie et al. have recently reported an elegant method to prepare chiral PMO materials, employing a mixture of enantiomerically pure biphenyl bis-siloxane with non-chiral biphenyl bis-siloxane, although no application is reported [24].

Nonetheless, in most of the cases, the synthesis of the chiral periodic mesoporous organosilicas takes place through a procedure with multiple stages. As best, at least two steps are needed to achieve the chiral PMOs [19]. Previously, the organic synthesis of

* Corresponding author. Fax: +34 914887086.
E-mail address: rafael.garcia@urjc.es (R.A. Garcia).

0021-9517/$ - see front matter © 2010 Elsevier Inc. All rights reserved.
doi:10.1016/j.jcat.2010.07.003

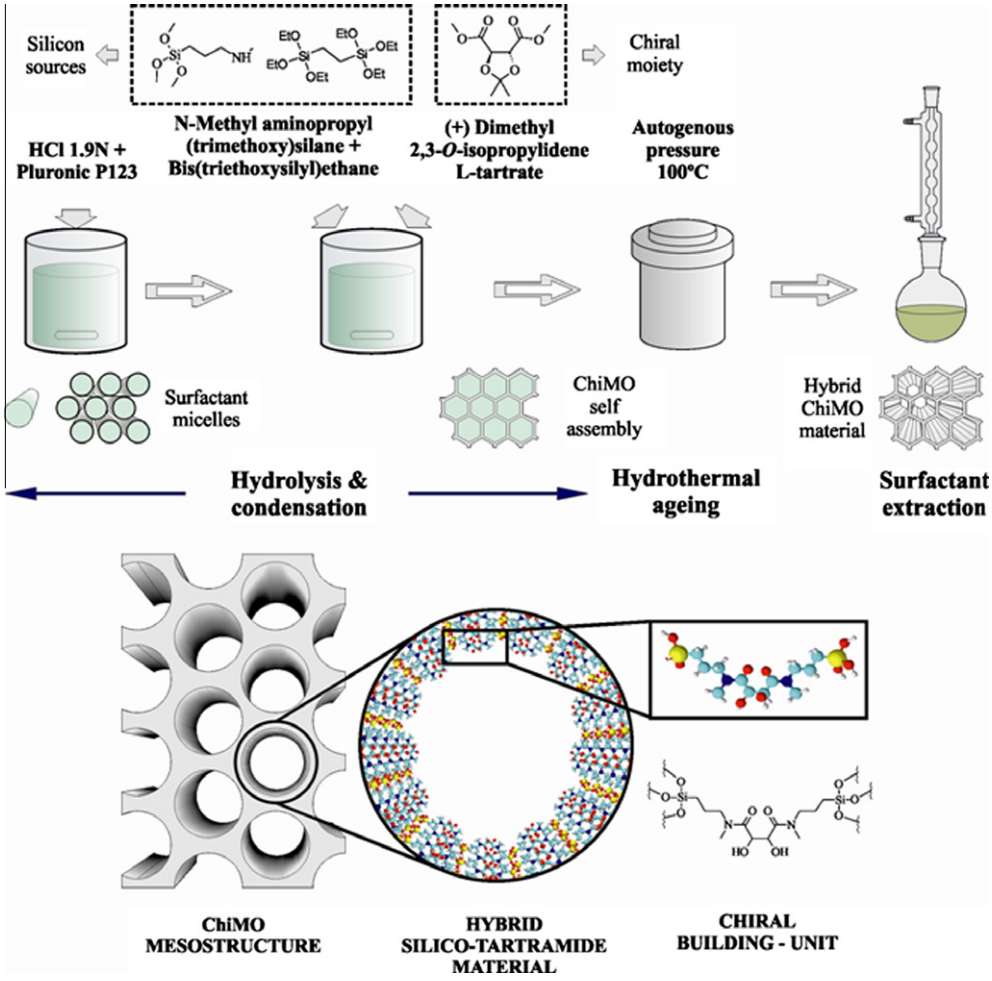

Scheme 1. One-pot synthesis of chiral PMO SBA-15-like material.

the, usually non-commercial, chiral bis-organosilane is performed following different reaction steps and further purification, with the subsequent assemblage of the chiral precursor around the templating micelles. This tedious drawback is circumvented by the procedure that we outline herein, in which a new, easy and unprecedented one-pot approach to the synthesis of chiral SBA-15-like material is accomplished, based on a tartrate-derived chiral precursor and a non-chiral bis-organosilane, 1,2-bis(triethoxysilyl)ethane. Interestingly, this chiral organic–inorganic material could be prepared from purely organic monomers, without the need of using silica sources, like TEOS, that lead to conventional inorganic silica, in the presence of Pluronic 123 as templating agent under acidic conditions (Scheme 1). Besides, the chiral precursor loadings incorporated without distorting the mesoscopic structure are meaningfully higher than the previously reported works [11,16,25–27]. The so-obtained chiral PMOs exhibit a good activity and moderate enantioselectivity in the asymmetric sulfoxidation of thioanisole, confirming the inclusion of the chiral tartrate moiety into the inorganic silica framework.

2. Experimental

2.1. Chemicals

Pluronic P123 (PEO20-PPO70-PEO20; Aldrich), 1,2-bis(triethoxysilyl)ethane (BTSE, 99%, Aldrich), potassium chloride (KCl, 99%, Aldrich), hydrochloric acid (HCl, 35%, Scharlab), (N-methylaminopropyl)trimethoxysilane (GELEST), dimethyl-2,3-*O*-isopropylidene L-tartrate (DMT, ALDRICH) and ethanol (Scharlab) were used as received without further purification. Dichloromethane was distilled from P_2O_5 prior its use as solvent for the catalytic tests.

2.2. Synthesis of SBA-15 chiral periodic mesoporous organosilica

In a typical synthesis, 2 g of Pluronic P123 and 19.7 g of KCl were dissolved in 65 mL of 0.5 N hydrochloric acid in a round-bottom flask at room temperature. After complete dissolution, the mixture was warmed up to 40 °C, and 2.9 g of BTSE was added in a single step. After 1 h, (N-methylaminopropyl)trimethoxysilane and protected dimethyltartrate were added in order to obtain the bis-silylated tartramide through an *in-situ* transamidation reaction. Different materials were prepared in the molar range of BTSE to tartramide from 100:0 to 30:80. The solution was then vigorously stirred for 20 h at 40 °C and hydrothermally aged at 100 °C for another 24 h. The product was then recovered by filtration before being air-dried. The surfactant removal consisted of an extraction step with ethanol. Typically, 1 g of as-made material was treated with 100 mL of ethanol under reflux overnight. The solids were then recovered by filtration while still warm and thoroughly washed with fresh ethanol before air-dried.

2.3. Characterization

The so-prepared materials were characterized by means of different analytical techniques. Nitrogen adsorption–desorption isotherms were collected at 77 K using a Micromeritics TriStar 3000

unit. Previously, the samples were outgassed at 200 °C for 4 h under nitrogen flow. The surface area measurements were performed according to the BET method from nitrogen adsorption points in the range $P/P_0 = 0.05–0.2$. Pore size distribution was determined applying the Barrett–Joyner–Halenda model (BJH) to the adsorption branch of the isotherm, assuming cylindrical pore geometry. For each sample, the average pore size was estimated as the diameter corresponding to the maximum of the pore size distribution curve. Total pore volume was taken at a relative pressure P/P_0 of 0.985

X-ray powder diffraction patterns were collected on a Philips X'pert diffractometer equipped with an accessory for low-angle measurements. XRD analyses were recorded using the Cu Kα line in the 2θ range from 0.5° to 10° with a step size of 0.02° and a counting time of 10 s.

FTIR analyses were collected, using the KBr buffer technique, on a Mattson Infinity series apparatus in the wavelength range from 4000 to 400 cm^{-1} with a step size of 2 cm^{-1} and collecting 64 scans for each analysis. The samples were also placed in a catalytic chamber HVC-DPR (Harrick Scientific Company) where they were heated at different temperatures under vacuum (<10–4 mbar) with a 1.5 °C/min heating rate.

Solid-state ^{13}C and ^{29}Si MAS NMR experiments were performed on a Varian Infinity 400 MHz spectrometer fitted with a 9.4 T magnet. These nuclei resonate at 100.53 and 79.41 MHz, respectively. An H/X 7.5 mm MAS probe and ZrO_2 rotors spinning at 6 kHz were used. On CP experiments, the cross-polarization time was determined to guarantee the total proton polarization verifying the Hartmann–Hann condition. For ^{13}C acquisition, $\pi/2$ pulse, number of scans, repetition delay and contact time were 4.25 μs, 2000 scans, 3 s and 1 ms, respectively. The ^{29}Si CP experiments were performed for 3000 scans, $\pi/2$ pulse of 3.5 μs and 15 s of repetition time, while the contact period was 10 ms since cross-polarization depends upon heteronuclear dipolar interaction, the greater distance the larger cross-polarization time. ^{13}C and ^{29}Si chemical shifts were externally referenced to adamantane and tetramethylsilane, respectively.

2.4. Catalytic tests

Reaction tests for the asymmetric oxidation of sulfides were carried out under a nitrogen atmosphere using standard Schlenk techniques (Scheme 2). The PMO used as solid chiral ligand was previously outgassed and dried in a Kugelrohr apparatus at 130 °C under vacuum (1 torr) overnight before being employed in the catalytic tests. Inert conditions were ensured by passing a continuous nitrogen stream through the reactor, which was maintained during the overall operation. Freshly distilled dichloromethane (50 mL) was then transferred into the reactor via syringe, and the mixture was magnetically stirred. Titanium isopropoxide (0.056 mmol) and 2-propanol (0.224 mmol) were added drop by drop to the resultant suspension. The mixture was then aged for 2 h in order to promote the contact between the titanium species and the chiral ligand sites present in the PMO material. After the aging step, both cumyl hydroperoxide (CHP, 0.56 mmol) and thioanisole (0.56 mmol) were added separately by dropping onto the catalytic suspension. Sample aliquots were collected in order to assess the evolution of the reaction. The mixture was allowed to react for 24 h.

3. Results and discussion

The mesostructured organosilicas with chiral ligands incorporated into the framework were obtained following a new and easy methodology, the procedure being represented in Scheme 1. Once the chiral tartrate derivative employed as chiral precursor, protected L-(+)-dimethyl tartrate (DMT), is mixed with the (N-methyl-3-aminopropyl)trimethoxysilane under the weak acidic conditions needed for synthesizing a SBA-15-like framework material, a transamidation reaction takes place, leading to the bis-silylated chiral precursor. Besides, the presence of 1,2-bis(triethoxysilyl)ethane (BTSE) and the copolymer Pluronic P123 triblock copolymer provides the mesoscopic ordering to the final material. Therefore, during the *in-situ* transamidation reaction, the hydrolysis of the chiral and non-chiral bis-organosilane silica precursors and the condensation of these latter species around micelles formed by the structure-directing agent are readily accomplished leading to a chiral PMO material.

After the optimization of the aging time and the hydrolysis and condensation stage, the progressive incorporation of higher amounts of protected DMT was carried out. Thus, Table 1 summarizes the physico-chemical properties of the obtained chiral PMOs.

Fig. 1 shows the N_2 adsorption–desorption isotherms for the synthesized materials. BET surface, pore size distribution (inset in Fig. 1) and total pore volume are obtained by processing the adsorption branch of the collected isotherm data. Chiral PMO-10, 20, 30 and 50 materials show type IV nitrogen adsorption–desorption curves, according to the IUPAC classification, which are typical of mesoporous solids. The steep adsorption step detected around $P/P_0 = 0.65–0.70$, corresponding to the capillary condensation of nitrogen in uniform pores, evidences the formation of well-structured solid materials with narrow pore sizes distributions, as it is derived from the BJH analysis shown in the onset. On the other hand, the ordering degree seems to be influenced by the content of the organic functionality. Although the width of the pore size distributions seems not to be greatly modified, the area below the pore size distribution, which is the total pore volume, or at least the mesopore volume, decreases when increasing the organic ligand loading. Besides, the mean pore size is slightly shifted to lower values because of the same reasons already exposed. Finally, chiral PMO-70 exhibits a negligible yield to solid, indicating that higher loadings of bis-organosilane inhibit the formation of these materials. Thereby, a significant amount of BTSE must coexist in the media besides the chiral precursors to provide enough mesoscopic ordering to the final chiral PMO SBA-15-type materials. Nevertheless, chiral periodic mesoporous solid materials with a ratio BTSE/DMT as high as 50:50 have been synthesized, which, according to the earlier reports, is the highest organic chiral loading incorporated into the three-dimensional structure of a PMO material, to the best of our knowledge. Although for this 50:50 precursor mixture, the incorporation of chiral functionality suffers a slight decline compared to sample S20, as shown in Table 1 (HCNS column), it is still high enough and the material sufficiently ordered, as to endorse the previous comment.

Fig. 2 displays the XRD patterns of the template-free synthesized chiral PMOs at increasing chiral organic precursor loadings. The presence of the characteristic diffraction at $2\theta = 0.8–0.9°$, corresponding to the d_{100} basal plane of SBA-15-type materials, confirms the formation of a mesoporous structure for those solids. These materials preserve the periodic structure even after template P123 removal by washing with ethanol, related probably to the beneficial action of hydrothermal treatment during the framework consolidation.

As displayed in Table 1, a reduction in the BET surface area and pore size diameter occurs as the chiral organic precursor loading is increased. Additionally, and excepting the PMO-10 sample that shows a slight decrease, the general trend points out to wall thickness reinforcement as the pore size diameter declines, which is in accordance with results previously described for other PMO materials [14]. The observed tendency may provide an idea of the importance of the organic moiety in the final materials ordering.

Table 1
Physico-chemical properties of chiral PMO.

Material	Organic %[a]	N_2 adsorption analysis			X-ray diffraction (Å)			HCNS	
		A_{BET}[b] ($m^2\ g^{-1}$)	D_p[c] (Å)	V_p[d] ($cm^3\ g^{-1}$)	d_{100}[e]	a_0[f]	Wt[g]	% N[h]	mmole tartramide/g material[i]
S0	0	572	64.50	0.75	103.85	119.92	55.42	–	–
S10	10	637	64.90	0.84	98.33	113.54	48.64	1.76	0.63
S20	20	460	58.20	0.63	107.48	124.11	65.91	4.53	1.62
S50	50	306	55.00	0.41	99.68	115.10	60.10	4.04	1.44
S60	60	76	58.80	0.39	110.67	127.79	68.99	1.65	0.59
S70	70	–	–	–	–	–	–	–	–

[a] Proportion of chiral tartramide precursor incorporated into the gel during the synthesis step in molar basis.
[b] Specific surface area calculated by the BET method.
[c] Pore size diameter calculated by the BJH method.
[d] Total pore volume registered at $P/P_0 = 0.985$.
[e] Interplanar spacing.
[f] Cell unit parameter calculated assuming hexagonal ordering.
[g] Wall thickness calculated as $Wt = a_0 - D_p$.
[h] Calculated by elemental analysis.
[i] Incorporation of the chiral functionality into the final material based on elemental analysis.

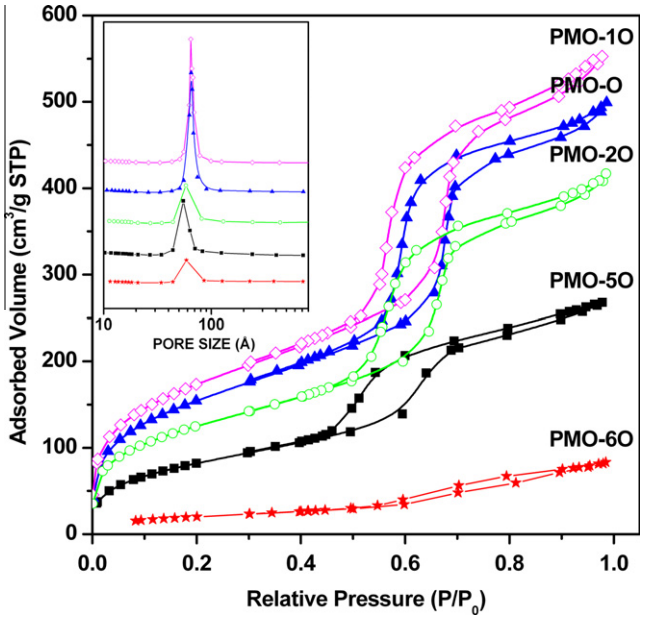

Fig. 1. N_2 Adsorption–desorption isotherms and pore size distribution (inset) for the synthesized chiral PMO materials.

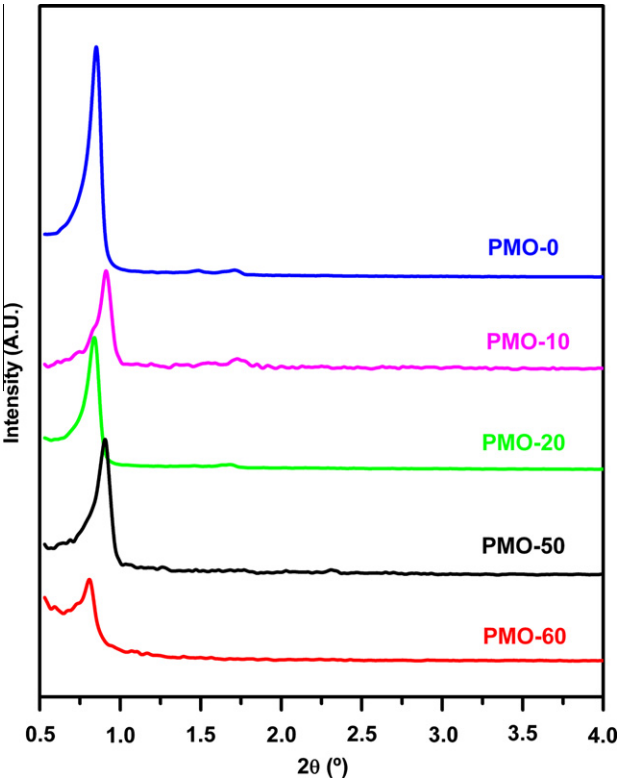

Fig. 2. XRD patterns obtained for chiral PMO materials with SBA-15-like structure.

Mesoscopic order is confirmed by TEM images (shown in Fig. 3) as definitive evidence of the structure ordering achieved on these chiral modified mesostructured materials. These samples show the typical honeycomb structure from SBA-15-type mesostructured materials.

A key point in the chiral PMO one-pot synthesis lies in the transamidation reaction between DMT and the organic tethering, providing the mixture of the latter with BTSE the capability of the assembly around micelles, in such a way the chiral silica formation may take place. To check the formation of this amide precursor, FTIR analyses of the chiral PMO samples were acquired at different treatment temperatures using a proper chamber as displayed in Fig. 4. At room temperature, an absorption band appears at around 1640 cm^{-1}, which could be assigned to an amide group formation but also to physisorbed water. Subsequently, the temperature was increased to 300 °C, and it was observed that the intensity of the absorption band showed almost no decrease as the outgassing temperature was increased, shifting to slightly lower wavenumbers, which undoubtedly supports the amide group formation. Additionally, a broad adsorption at around 3300 cm^{-1}, assigned to hydrogen-bonded SiOH groups perturbed by physically adsorbed water, is seen. With the increase in the outgassing temperature, the intensity of this band decreased and shifted to lower wavenumbers because of dehydration and dehydroxylation at higher temperatures in vacuum. Besides, the spectrum of the PMO-0 reference material synthesized from pure BTSE, without any chiral organic loading, showed complete absence of the signal at 1640 cm^{-1} at high temperatures in vacuum, which confirms the complete absence of adsorbed water in these conditions. Therefore, FTIR analyses yielded insight into the inclusion of the chiral organic species into the silica.

Accordingly, the incorporation of the organic species into the framework of mesostructured material was definitely corroborated by the ^{13}C NMR solid-state experiments. Fig. 5 shows the peak assignments corresponding to the different functionalities

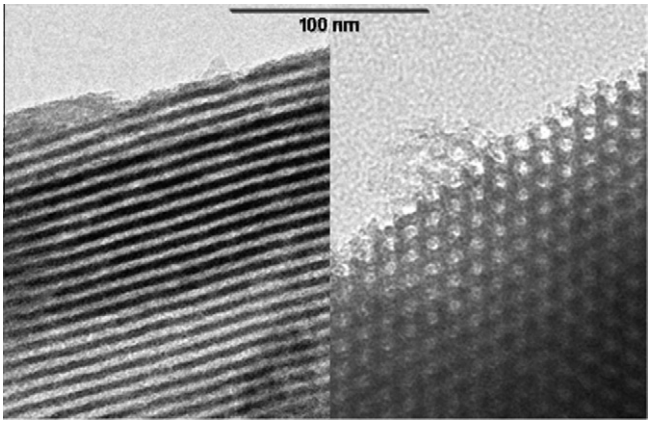

Fig. 3. TEM images recorded for sample PMO-50.

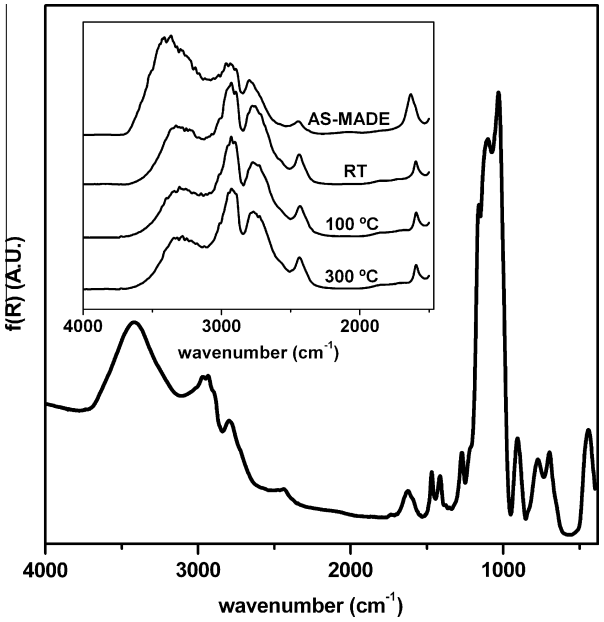

Fig. 4. FTIR spectra collected for sample PMO-50 at different temperatures.

incorporated into the silica-supported tartramide chiral species. The lower shielding chemical shift at about 180 ppm corresponds to quaternary carbons at the carbonyl groups, C═O, from the synthesized amide, though however the presence of two peaks denotes different tartramide environments. The signal centered at around 70 ppm corresponds to two chiral carbon atoms bonded to hydroxyl groups, *C*H—OH. This fact and the complete absence of the 130 and 104 ppm signals corresponding to the O-isopropylidene protecting group indicate that the deprotection of the chiral precursor ligand has been totally achieved. The signals centered at 32 and 51 ppm can be assigned to N*C*H_3 and N*C*H_2, respectively, which denotes the presence of the nitrogen atom in the material. Also, the two sharp peaks centered at 10 and 15 ppm were assigned to Si—*C*H_2 and Si—CH_2—*C*H_2, respectively. The spectrum shows two peaks centered at 20 and 59 ppm that could be related to the presence of the residual ethoxy groups coming from non-hydrolyzed ethoxide functionalities. Nevertheless, all these data confirm the presence of the immobilized tartramide organic precursor in the inorganic material framework.

Finally, ^{29}Si solid-state NMR was used to corroborate the presence of the chiral organic precursor and BTSE. The inset in Fig. 5 shows the ^{29}Si NMR spectrum of the chiral PMO-50 after P123 surfactant elimination, revealing the chemistry of the surface modification. The spectrum displays a main region centered at around −70 ppm. This pattern corresponds to species containing the chiral organic precursor, that is $(—O—)_3Si—R—Si(—O—)_3$, named T^n groups, where R denotes the chiral and non-chiral organic group, as previously confirmed by the ^{13}C NMR solid-state experiments. A large amount of cross-linked T^3 surface species, compared to T^2 and T^1 species, is formed, indicating that the level of condensation reached for these chiral materials is reasonably high. No presence of Q^n species is displayed in the spectrum, which confirms that no carbon—silicon bond cleavage occurred during the synthesis.

To evaluate the catalytic properties of the obtained chiral PMOs, the asymmetric oxidation of thioanisole was employed as a test reaction, using the chiral PMO as "solid" asymmetric ligand for the induction of enantioselectivity into the final product (Scheme 2). Asymmetric sulfoxides are very useful auxiliaries in asymmetric synthesis as chiral building blocks in multistep synthesis or as biologically active compounds [28,29]. The best homogeneous conditions were fixed for the reaction, so a molar combination of $Ti(O^i—Pr)_4$/chiral tartramide/i-PrOH 1:4:4 was chosen (Kagan catalyst) as initial conditions for the heterogeneous oxidation reactions. Cumyl hydroperoxide was used as oxidizing agent because of the better performance of this oxidant in asymmetric sulfoxidation, with the initial $Ti(O^i—Pr)_4$/CHP molar ratio of 1:20. Under these conditions, and for comparison purposes, the reaction employing the homogeneous catalytic system formed by titanium isopropoxide, L-(+)-diisopropyl tartrate and isopropanol was accomplished. This catalytic system led to a very high substrate conversion after reacting for 24 h (92%), inducing an enantiomeric excess over the final product of 94% ee. With regard to the heterogeneous system presented in this work, the selected sample to carry out the test reaction was the PMO-50 material, due to the high tartramide incorporation in its structure (see Table 1), and to the adequate textural properties showed by this sample. A blank reaction was performed, as reference, in the presence of chiral PMO-50 but in the absence of any titanium source. In this way, neither appreciable substrate conversion nor induced enantioselectivity was accomplished, even for a long reaction time of 24 h. The influence of different variables on the activity and enantioselectivity of the chiral PMO has been studied: two of the more crucial ones are CHP/Ti and DMT/Ti molar ratio as is shown in Fig. 6. The CHP/Ti molar ratio was the first optimized variable in order to reduce the sulfone formation during the reaction, keeping constant the other molar ratio in the homogeneous conditions values for all the experiments performed. This is a crucial operating variable, since slight variations cause large differences in the sulfone concentration obtained as secondary reaction product (Scheme 1). These studies have established the optimal CHP/Ti molar ratio around 10/1, higher values lead to a dramatic decrease in the sulfoxide formation due to the higher amount of sulfone obtained. Once the CHP/Ti molar ratio was fixed, the influence of the tartrate/titanium molar ratio on the activity and enantioselectivity of the reaction was checked. This variable influences on the distribution of the population of different catalytic species in the reaction media. It appears that there is an optimal value for the 16:1 ratio. Below this value, enantioselectivity decreases rapidly, because of a deficiency in chiral ligand, whereas beyond this molar concentration, both catalytic activity and enantioselectivity diminish, probably because of a saturation of the coordination positions to the metallic center, making the access to reactants difficult.

With regard to the catalytic behavior of the chiral PMO-50 material prepared, increasing sulfoxide yields are achieved for longer reaction times, while the enantiomeric excess induced into the final sulfoxides is kept constant during the overall reaction process around 30% ee (60% and 71% sulfoxide yield at 3 and 24 h, respectively), being similar to the values achieved with other

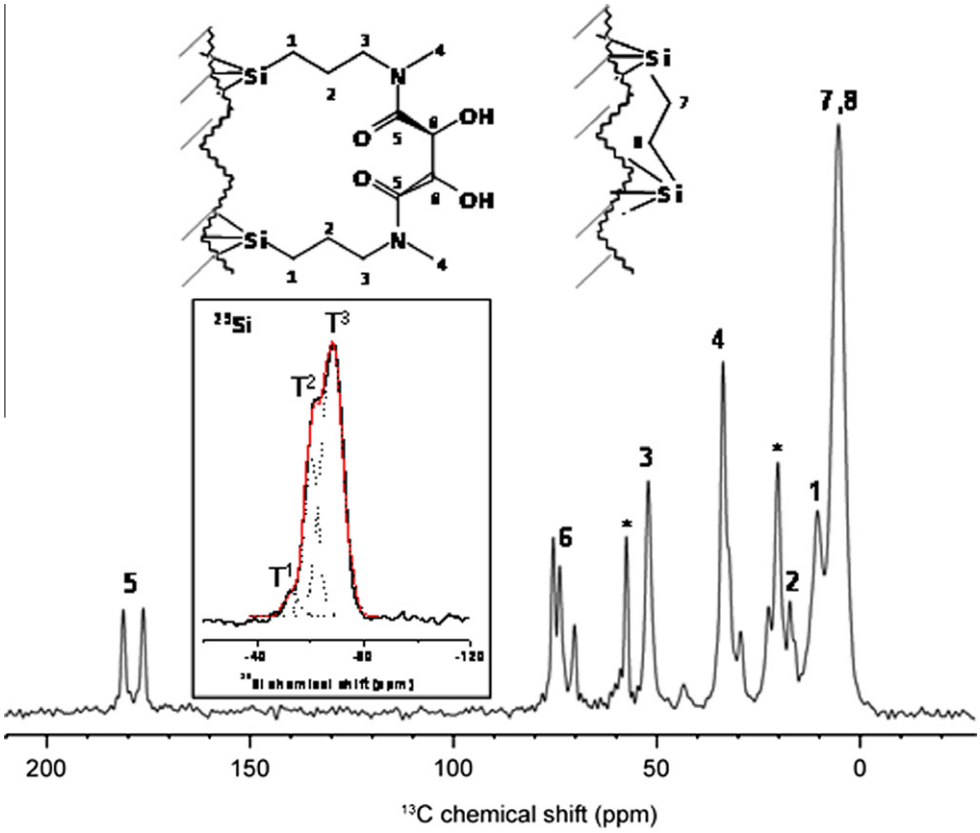

Fig. 5. ^{13}C CP-MAS solid-state NMR spectrum of the chiral PMO-50 sample. In the inset, the ^{29}Si CP-MAS solid-state NMR spectrum corresponding to the same sample is sketched. Asterisks correspond to the residual ethoxy functionalities.

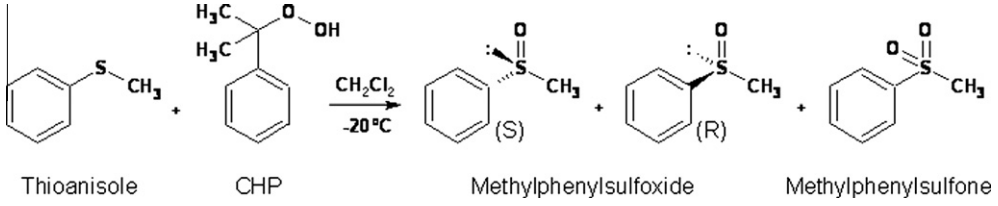

Scheme 2. Catalytic test: asymmetric oxidation of methyl phenyl sulfide (thioanisole).

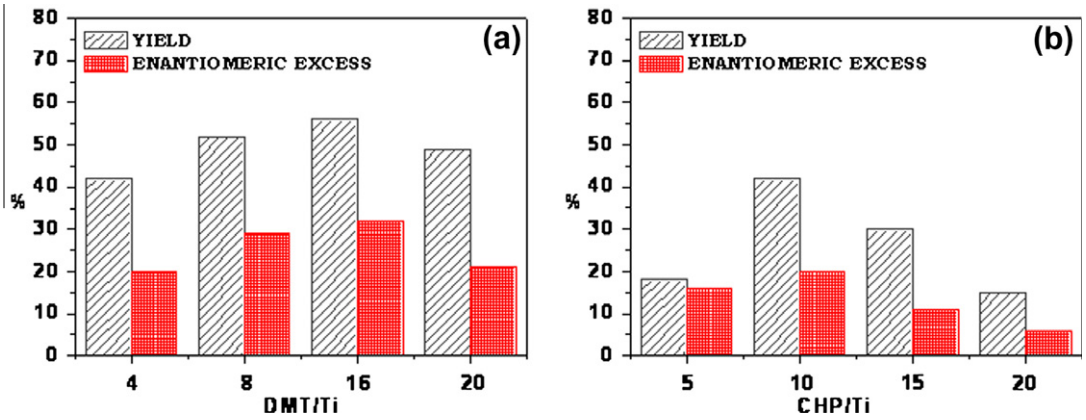

Fig. 6. Representation of the effect of CHP/Ti (a) and DMT/Ti (b) molar ratio influence on the yield and the enantiomeric excess in the thioanisole asymmetric oxidation.

heterogeneous chiral precursors either on the same or on different asymmetric synthesis [11,14]. On the other hand, the chiral PMO has been successfully reused as solid chiral ligand in the sulfoxidation reaction. In this case, lower sulfoxide yields are achieved, whereas the induced enantioselectivity over the sulfoxide is maintained at a similar level to that obtained for the fresh catalyst. These results confirm the heterogeneous behavior of the organic chiral tartramide moieties as chiral periodic mesoporous organosilica.

4. Conclusions

As conclusions, we have demonstrated the successful synthesis of a chiral PMO SBA-15-type material synthesis, from 100% purely organic monomers in the absence of TEOS, by an easy one-pot methodology, in which the chiral and non-chiral organosilica precursors are assembled, both together, around the non-ionic surfactant. Chiral periodic mesoporous solid materials with a precursor mixture ratio BTSE/DMT as high as 50:50, without any measurable decline in the textural properties such as the materials' ordering, have been synthesized. Additionally, large incorporation of chiral functionalities up to 1.62 mmole tartramide/g has been reached. Likewise, FTIR and NMR solid-state techniques confirm the presence of the chiral organic precursor in the SBA-15-type material framework. The thioanisole asymmetric oxidation reaction has been used to validate the heterogeneously synthesized catalyst activity, achieving enantiomeric excess (ee) and yield to sulfoxide up to 30% and 71%, respectively. Finally, this approach afford a new synthesis route for researchers trying to gain understanding on the investigation into heterogeneous asymmetric synthesis, glimpsing the potential applications of this method from the point of view of incorporating not only tartramide moieties but other homogeneous chiral auxiliaries into the three-dimensional mesostructure of organic–inorganic silica support (chiral PMOs materials) in only one step, which would mean a higher overall throughput than the more tedious procedures previously reported, in which the organic chiral precursor has to previously prepared, separated and purified and subsequently added in a second step to the inorganic support synthesis media. Thus, not only Sharpless chiral auxiliary, but BINOL and derivatives, Mn-Salen, etc. are susceptible to be heterogeneized following this methodology, being part of the PMO silica wall structure.

Acknowledgment

The financial support of the Spanish government (CTQ2008-05909/PPQ) is gratefully acknowledged.

References

[1] T. Asefa, M.J. MacLachlan, N. Coombs, G.A. Ozin, Nature 402 (1999) 867–871.
[2] S. Inagaki, S. Guan, Y. Fukushima, T. Oshuna, O. Terasaki, J. Am. Chem. Soc. 121 (1999) 9611–9614.
[3] J. Melde, B.T. Holland, C.F. Blanford, A. Stein, Chem. Mater. 11 (1999) 3302–3308.
[4] S. Inagaki, S. Guan, T. Ohsuna, O. Terasaki, Nature 416 (2002) 304–307.
[5] S. Bracco, A. Comotti, P. Valsesia, B.F. Chmelka, P. Sozzani, Chem. Commun. (2008) 4798–4800.
[6] K. Landskron, G.A. Ozin, Science 306 (2004) 1529–1532.
[7] O. Olkhovyk, M. Jaroniec, J. Am. Chem. Soc. 127 (2005) 60–61.
[8] W. Whitnall, L. Cademartiri, G.A. Ozin, J. Am. Chem. Soc. 129 (2007) 15644–15649.
[9] G. Morales, G.L. Athens, B.F. Chmelka, R. Van Grieken, J.A. Melero, J. Catal. 254 (2008) 205–217.
[10] C. Baleizao, B. Gigante, D. Das, M. Álvaro, H. Garcia, A. Corma, Chem. Commun. (2003) 1860–1861.
[11] D. Jiang, Q. Yang, H. Wang, G. Zhu, J. Yang, C. Li, J. Catal. 239 (2006) 65–73.
[12] M. Alvaro, M. Benitez, D. Das, B. Ferrer, H. García, Chem. Mater. 16 (2004) 2222–2228.
[13] C. Li, D. Jiang, Q. Yang, H. Wang, G. Zhu, J. Yang, J. Catal. 239 (2006) 65–73.
[14] R.A. García, R. Van Grieken, J. Iglesias, V. Morales, D. Gordillo, Chem. Mater. 20 (2008) 2964–2971.
[15] Q. Yang, Jian Liu, L. Zhang, C. Li, J. Mater. Chem. 19 (2009) 1945–1955.
[16] H. Garcia, M. Benitez, G. Bringmann, M. Dreyer, H. Ihmels, M. Waidelich, K. Wissel, J. Org. Chem. 70 (2005) 2315–2321.
[17] L. Zhang, J. Liu, J. Yang, Q. Yang, C. Li, Chem. Asian J. 3 (2008) 1842–1849.
[18] T.P. Nguyen, P. Hesemann, P. Gaveau, J.J.E. Moreau, J. Mater. Chem. 19 (2009) 4164–4171.
[19] A. Ide, R. Voss, G. Scholz, G.A. Ozin, M. Antonietti, A. Thomas, Chem. Mater. 19 (2007) 2649–2657.
[20] X. Meng, T. Yokoi, D. Lu, T. Tatsumi, Angew. Chem. Int. Ed. 46 (2007) 7796–7798.
[21] S. Inagaki, S. Guan, Q. Yang, M.P. Kapoor, T. Shimada, Chem. Commun. 2 (2008) 202–204.
[22] S. Polarz, A. Kuschel, Adv. Mater. 18 (2006) 1206–1209.
[23] J. Morell, S. Chatterjee, P.J. Klar, D. Mauder, I. Shenderovich, F. Hoffmann, M. Fröba, Eur. J. Chem. A 14 (2008) 5935–5940.
[24] S. MacQuarrie, M.P. Thompson, A. Blanc, N.J. Mosey, R.P. Lemieux, C.M. Cathleen, J. Am. Chem. Soc. 130 (2008) 14099–14101.
[25] P. Wang, J. Yang, J. Liu, L. Zhang, Q. Yang, Micropor. Mesopor. Mater. 117 (2009) 91–97.
[26] G. Zhu, H. Zhong, Q. Yang, C. Li, Micropor. Mesopor. Mater. 116 (2008) 36–43.
[27] T. Yokoi, Y. Yamataka, Y. Ara, S. Sato, Y. Kubota, T. Tatsumi, Micropor. Mesopor. Mater. 103 (2007) 20–28.
[28] P. Pitchen, H.B. Kagan, Tetrahedron Lett. 25 (1984) 1049–1055.
[29] J.M. Brunel, H.B. Kagan, Synlett 4 (1996) 404–406.